

文章编号:1000-8055(2014)10-2402-08

doi:10.13224/j.cnki.jasp.2014.10.017

# Numerical investigation of windage heating within shrouded rotor-stator cavity system with central inflow

WANG Qian-shun, ZHANG Da, LUO Xiang, XU Guo-qiang

(National Key Laboratory of Science and Technology on Aero-Engine Aero-thermodynamics,  
School of Energy and Power Engineering,  
Beijing University of Aeronautics and Astronautics, Beijing 100191, China)

**Abstract:** The rotating disk surface temperature rise due to windage heating effect by numerically modeling the turbulent flow within a rotor-stator cavity which is available with a peripheral shroud and imposed through airflow was dealt with. The windage heating may be defined as viscous friction heating caused by relative velocity differences across the boundary layers between the fluid and the rotating disk surface. The kinetic energy dissipation process could transform the rotating shaft power into thermal heating. Commercial finite volume based solver, ANSYS/CFX was employed to numerically simulate this physical process by using the shear stress transport (SST) turbulence model. CFD results include the rotating disk surface temperature axial distribution and tangential velocity distribution of the fluid domain. The velocity difference between the result obtained by particle image velocimetry (PIV) experiments and CFD simulation are within 5%. The adiabatic disk temperature rise can be calculated by the tangential velocity of disk and fluid in large gap ratio and turbulent parameter. CFD temperature distribution results and those estimated via velocity differences are within 10%.

**Key words:** windage heating; rotor-stator cavity system; flow structure; recovery temperature;

**CLC number:** V231

**Document code:** A

## Nomenclature

$Re_\phi$	Rotating Reynolds number	$G$	Gap ratio
$T_0$	Flow temperature, K	$G_c$	Shroud clearance ratio
$C_w$	Non-dimensional flow rate	$r_{rev}$	Temperature recovery coefficient
$T_{rev}$	Recovery temperature, K	$\beta$	Swirl ratio
$Pr$	Prandtl number	$V_c$	Tangential velocity of flow core, m/s
$T_{in}$	Inlet temperature, K	$r$	Radius, m
$\lambda_t$	Turbulent parameter	$c_p$	Specific heat at constant pressure, J/(kg/K)
$\Delta T$	Temperature rise, K		

As to shrouded rotor-stator cavity systems, the fluid flow and heat transfer have been the subject of a great number of studies for the gas turbine applications. The windage loss caused by the friction between the cooling air and the rotating disk become quite serious as the rotating

speed of the disk becomes high. Frictional heating on the rotor surface due to windage losses are particularly important for the life span of the disk and downstream coolant parameter. But the designer knows that too little coolant will result in hotter disk temperatures and reduce parts life

while too much flow may harm engine overall performances. A balance should be achieved between engine performance and parts life by running an analytical model with varying amounts of cooling flow rates and estimating disk temperatures.

Daily and Nece<sup>[1]</sup> established empirical correlations about the frictional torque characteristics for rotor-stator cavity system without radial outflow, the magnitude of rotating Reynolds numbers  $Re_\varphi$  is up to  $10^7$ . Bayley and Owen et al<sup>[2-6]</sup> had systematically researched the torque coefficient of rotor-stator cavity system, and found the influence discipline to heat transfer caused by windage heating with different disk surface temperature types. Coren and Child et al<sup>[7-8]</sup> presented experimental data and an associated correlation for the windage rise resulting from a disk rotating in air. A test rig had been developed that used an electric motor to drive a smooth bladeless rotor inside an enclosed pressurized housing. Liu et al<sup>[9]</sup> made a prediction of windage losses of an enclosed high speed composite rotor in low air pressure environment. Da Soghe et al<sup>[10]</sup> made an analysis of gas turbine rotating cavities by a one-dimensional model.

For shrouded rotor-stator cavity system, the flow structure has a popular belief as the Batchelor-Stewartson model<sup>[10-12]</sup>. In 1950s, Batchelor et al<sup>[13-15]</sup> proposed a model which assumes that there is a rotating core of fluid between the rotating disk and the stator, with a relatively stable angular velocity value less than the disk. In this model, the boundary layer on the rotor has a velocity gradient which could be considered from the rotational speed of rotor to core with the no-slip condition.

The study of this paper tries to testify and introduce a method which could be used to estimate the windage heating characteristics of a shrouded rotor-stator cavity system. It shows that the windage heating on the rotor surface is affected by the tangential velocity difference between the rotating disk and the rotating fluid core. For simplification of analysis, the flow speed of the core may be considered the tangential

velocity of the fluid which at axial middle section in the cavity. With the influencing discipline of the rotating Reynolds number, gap ratio and non-dimensional flow rate, the variation of turbulent parameter within the cavity will exert a direct influence upon the flow structure and then the velocity gradient of the boundary layers between the fluid and the rotor surface. Since the windage heating intensity depends upon the strength of viscous friction inside the boundary layer, the tangential velocity distribution of the fluid of the middle axial cross-section becomes a significant parameter. This velocity difference could be used to calculate the recovery temperature of the fluid near the rotating disk using the heat transfer theory of high speed air. It can be extended to the rotor-stator cavities in the real gas turbine machines to estimate the temperature boundary conditions of heat transfer of the turbine disk.

## 1 Description of research approach

### 1.1 Geometrical configurations

The sketch of the rotor-stator cavity system considered in the present study is illustrated in Fig. 1. Four different gap sizes are designed to simulate four different gap ratios of the rotor-stator cavity system. All cavities are composed of a smooth surface rotating disk and a smooth stationary disk. The superimposed fluid to simulate the centrifugal cooling air in the turbine machine, enters the cavity axially through the central pipeline on the stator, then flows along the radius and exits this cavity through the rotor-stator gap at the high radius.

These geometrical dimensions of all three configurations are showed in Table 1:  $b$  is the radius of the rotating disk;  $r_1$  is the radius of the central inlet for the inflow;  $s$  is the axial distance between the rotor and stator  $s_c$  is the axial distance between the shroud and rotor. The gap ratio of the cavity  $G$ , shroud clearance ratio  $G_c$ , rotating Reynolds number  $Re_\varphi$  and the non-dimensional flow rate  $C_w$  which mainly control the flow structure are defined as follows:

$$G = \frac{s}{b} \quad G_c = \frac{s_c}{b} \quad Re_\varphi = \frac{\rho \omega^2 r}{\mu} \quad C_w = \frac{\dot{m}}{\mu R} \quad (1)$$

where  $\omega$  is the angular rotational speed of the rotor,  $\mu$  is the dynamic viscosity of the fluid and  $\dot{m}$  is the superimposed inflow rate.

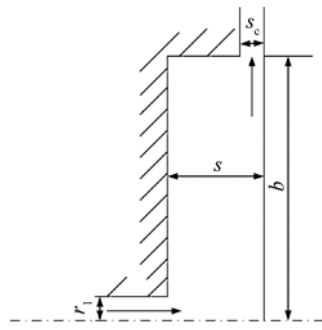


Fig. 1 Sketch of the rotor-stator cavity system considered in the present study

**Table 1 Geometric dimensions of the shrouded rotor-stator cavity**

$b/\text{m}$	$r_1/\text{mm}$	$s/\text{mm}$	$s_c/\text{mm}$
0.225	20	4.5 13.5 27.0 40.5	1

## 1.2 Numerical method

Three-dimensional models have been simulated by using commercial software of CFD (Fig. 2), ANSYS/CFX in this paper for predicting the steady flow in the cavity of shrouded rotor-stator cavity system. Flow structures and rotor surface temperature distributions have been obtained under different testing conditions. The turbulence model is SST model for a compressible perfect flow. The size of the first floor grid near the wall is set as  $10^{-6}\text{ m}$  to improve the calculation precision in boundary layers. It should be noted that the viscous work term in energy equation must be checked before calculation; otherwise the windage heating effect can't be reflected in truth.

The boundary conditions are set as follows: the rotational speeds of the rotor are 8000 r/min and 12000 r/min. At the inlet, the mass flow is

set between 100 kg/h to 500 kg/h. Calculated from the variables above, rotating Reynolds number and non-dimensional flow rate are displayed in Table 2. In the outflow section, the pressure is constant as  $10^5\text{ Pa}$ . The fluid temperature at the inlet is set as 300 K. All surfaces in the model (rotor, stator, inlet and shroud) are heat insulation and hydraulically smooth, to simulate a disk which has an adiabatic heat boundary condition without axial heat transfer.

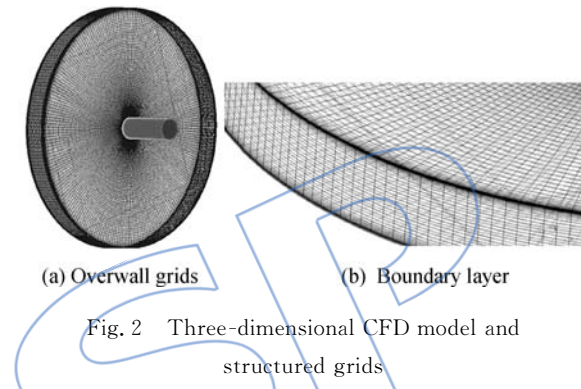


Fig. 2 Three-dimensional CFD model and structured grids

**Table 2 Non-dimensional parameters in CFD model**

$G$	$Re_\varphi/10^6$	$C_w/10^4$
0.02		0.682
0.06	2.82	2.040
0.12	4.23	3.410
0.18		

## 1.3 Experimental techniques

Particle image velocimetry (PIV) experiments have been performed to examine the accuracy of the acquired tangential velocity distribution by CFD. It can obtain the information of the flow field structure within the cavity of rotor-stator cavity systems, especially the tangential velocity distribution of the rotating fluid core between the rotor and stator. The major experimental apparatus (Fig. 3) comprises a titanium-alloy-made rotating disk driven by an adjustable-speed electric motor, which has a maximum rotational speed of 15 000 r/min. The stator and shroud is made of transparency organic glass to allow the laser go through. The sizes of the rotating disk, stationary disk and axial gap are the same as these in the CFD. The location of the sheet laser has the

same distances to rotor and stator to ensure that the rotating core can be captured by the high speed CCD (charge coupled device) camera. The core is assumed to be located at the middle axial position. And current numerical studies support this assumption. The CCD camera lens is perpendicular to the stator surface with a visible range which could cover the whole radius from the inlet pipe to the disk rim. With trace particle mixed in the superposed flow, the PIV system can measure the tangential velocity of fluid core distribution of the fluid along the radius (Fig. 4). The experimental results will be used to examine the accuracy of CFD results.

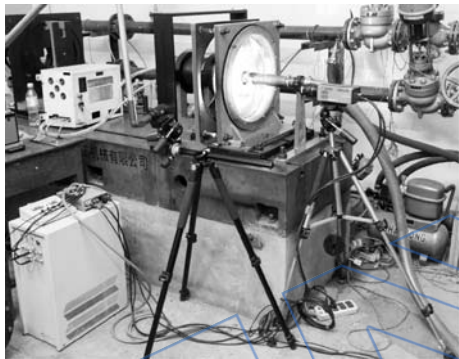


Fig. 3 General view of the experimental apparatus

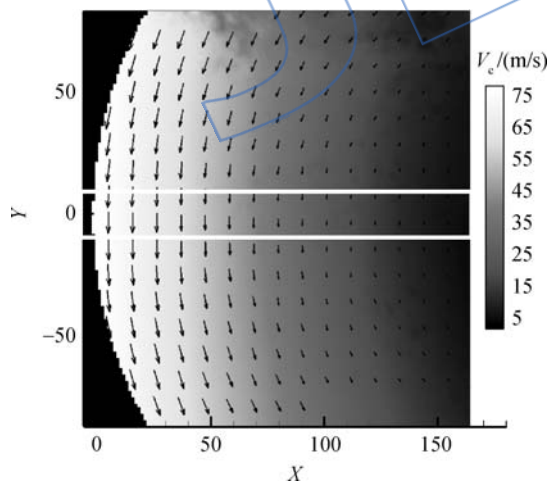


Fig. 4 Tangential velocity of flow core distribution obtained by PIV system in case of  $G=0.18$ ,  $Re_\varphi=4.23\times 10^6$ ,  $C_w=2.040\times 10^4$

## 2 Results and discussion

### 2.1 Fluid flow

With the experimental method introduced

above, the tangential velocity of flow core distribution map (Fig. 4) of the fluid has been acquired. These maps are the actually time average of 100 high speed double-patterning photos from the CCD camera. It should be noted that the map does not cover the whole rotor surface and the velocity contour is not circumferentially symmetrical. The reason is that the tracer particle near the uppermost or lowermost edges in the visible range can't be captured by two high speed CCD cameras at the same time. It has a negative influence for the calculation of velocity distribution so that the tangential velocity of flow core in the middle rectangular frame of the map (white outlined area in Fig. 4) is reasonable and more precise. A narrow rectangular region which covers the whole radial range of the two-dimensional velocity map is set to extract the radial distribution function curve of the tangential velocity of flow core. This curve would be compared with the results from the CFD results. Note that the range of dimensionless radius of experimental results is from 0.19 to 0.89.

Figure 5 shows the experimental and numerical tangential velocity of flow core distributions in a shrouded rotor-stator cavity system. Two kinds of results are well fitted, with equal curve extreme value or tendency. For the restrictions in experimental conditions, the situation of gap ratio less than 0.18 can't be operated, or else the disk surface near laser plane would result in great errors. Because of this,

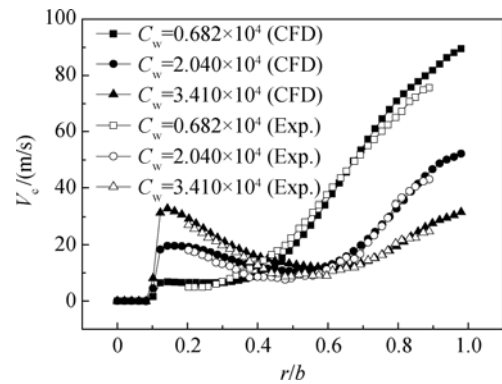


Fig. 5 Tangential velocity of flow core distribution obtained by CFD and experiments in case of  $G=0.18$ ,  $Re_\varphi=4.23\times 10^6$

the difference increases when the rotor-stator gap decreases. In general, the CFD results are in acceptable agreement with the PIV experimental results. That means the CFD results are precise enough in calculating the flow field and hence the other parameters.

## 2.2 Temperature distribution

The CFD results also contain the rotor surface temperature distributions. Besides, the velocity differences between the rotor surface and the rotating core can be used to estimate the recovery temperature rise. As it is supposed that the surfaces in this model are heat insulation, the temperature of the air near the wall is considered to be equal to the adiabatic wall temperature. The recovery temperature distribution can be calculated using heat transfer theory of high speed airflow. Since the CFD could predict the velocity values pretty well, the CFD temperature values are considered as comparison criteria. Then the estimated recovery temperature rises will be compared with the CFD results.

The recovery temperature distribution is calculated by the tangential velocity difference between the rotating core and the rotating disk. Then the calculated temperature rise is derived with the equation as follows:

$$\Delta T(r) = T_{\text{rev}}(r) - T_0(r) = r_{\text{rev}} \frac{[\omega r - V_c(r)]^2}{2c_p} \quad (2)$$

where  $T_0(r)$  is the local radius flow temperature;  $T_{\text{rev}}(r)$  is the recovery temperature near the rotating disk. The  $r_{\text{rev}}$  is calculated with Prandtl number  $Pr$  by equation as follows:

$$r_{\text{rev}} = Pr^{\frac{1}{3}} = \left( \frac{c_p \mu}{\lambda} \right)^{\frac{1}{3}} \quad (3)$$

where  $c_p$  is the specific heat at constant pressure of the air, and  $\lambda$  is the thermal conductivity.

The temperature rise  $\Delta T$  distributions comparison along the radius between the theoretical calculation and CFD is listed in Fig. 6. The gap ratio  $G$  here is 0.18, and the flow conditions ( $Re_\varphi$ ,  $C_w$ ) are varied.  $T_{\text{in}}$ , which is the inlet temperature is used to calculate the temperature rise because  $T_0(r)$  is unknown. In Fig. 6(a),

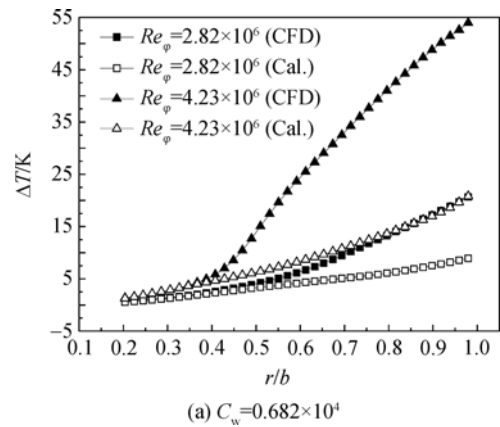
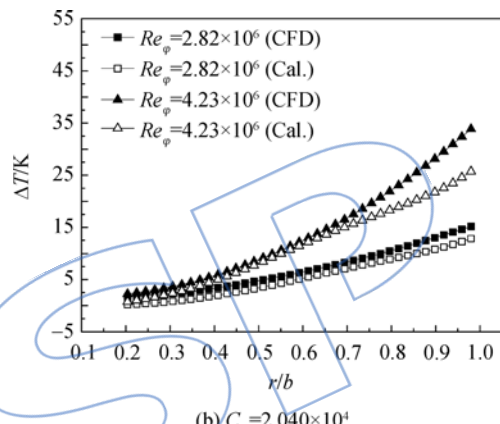
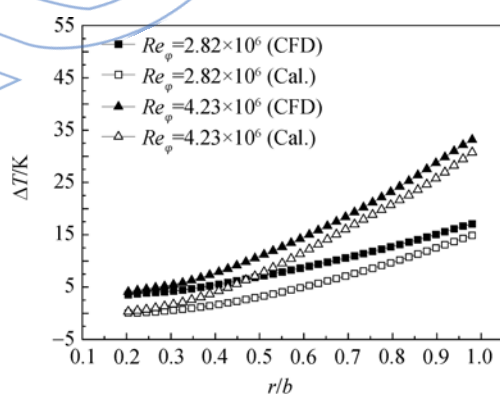
(a)  $C_w = 0.682 \times 10^4$ (b)  $C_w = 2.040 \times 10^4$ (c)  $C_w = 3.410 \times 10^4$ 

Fig. 6 Comparison results of temperature rise distribution by CFD and theoretical calculation on the surface of rotating disk, in case of  $G=0.18$ ,  $G_c=0.002$  and three non-dimensional flow rates

there is a great gap at high radius location ( $r/b > 0.4$ ) when the non-dimensional flow rate  $C_w$  is  $0.682 \times 10^4$ . With the non-dimensional flow rate increasing to  $2.040 \times 10^4$ , the difference between CFD result and theoretical calculation result decrease obviously. Once the non-dimensional flow rate reaches  $3.410 \times 10^4$ , two

curves get closer in high radial position with a gap of several degrees.

From the streamline chart in  $r-z$  section exported from CFD results (Fig. 7), the flow structure is clearly displayed which can explain the reason that the difference appears between two function curves.  $Re_\varphi$ ,  $C_w$  and  $\lambda_t$  for these situations are listed in Table 3. The  $\lambda_t$  is defined as

$$\lambda_t = \frac{C_w}{Re_\varphi^{0.8}} \quad (4)$$

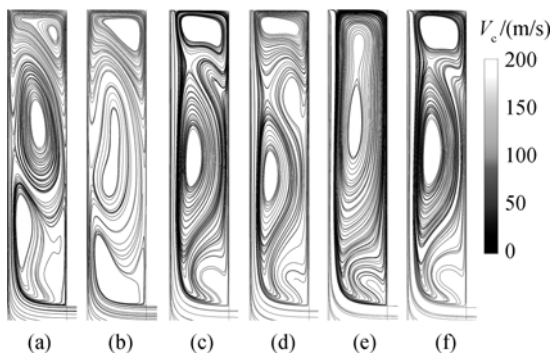


Fig. 7 Effects of the  $C_w$  and  $Re_\varphi$  in case of  $G=0.18$

Table 3 Flow parameters

Parameter	Flow structure					
	(a)	(b)	(c)	(d)	(e)	(f)
$Re_\varphi/10^6$	4.23	2.82	4.23	2.82	4.23	2.82
$C_w/10^4$	0.682	0.682	2.04	2.04	3.41	3.41
$\lambda_t$	0.034	0.047	0.102	0.141	0.170	0.236

From streamline charts with different parameters, it could be seen that there are strong vortices at higher radius when  $\lambda_t < 0.10$ . The inflow rate has a serious shortage to supply the radial outward flow rate caused by pumping effect. On one hand, the backflow which has already been heated due to the viscous friction may reheat the rotor surface. This is showed up as the mutational slope where  $r/b > 0.4$  in Fig. 6 (a). So the  $T_0(r)$  is inaccurate when it is replaced by  $T_{in}$ . On the other hand, the tangential velocity of the backflow shouldn't be considered as the mainstream speed of the boundary near the rotor because the angular momentum of the fluid is kept in the cavity by shroud. It leads to a high tangential velocity of flow core that causes a low

theoretical calculated temperature rise. The situation discussed above is quite extreme because the real turbine machine cooling air system used to prevent the phenomena of hot ingestion has  $\lambda_t$  larger than 0.06. So the situations depicted in Fig. 6 (b) and Fig. 6 (c) are most significant. The temperature rise difference in low radial position is caused by the windage heating effect of high radial velocity, especially in high non-dimensional flow rate in Fig. 6 (b) and Fig. 6 (c). But the absolute value of temperature rise in these situations which is much less than the one in high radial position can be ignored approximately in practical applications.

Fig. 8 shows the flow structure in different gap ratios with a turbulent parameter as 0.141, which is considered to be a suitable value for calculating the temperature rise more correctly when  $G=0.18$ .

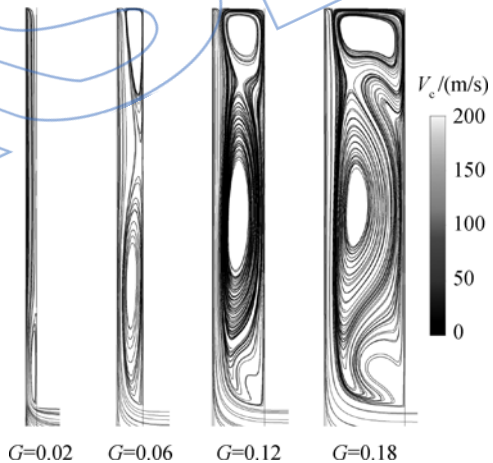


Fig. 8 Flow structure in different gap ratios of  $G=0.02, 0.06, 0.12$  and  $0.18$  in case of  $\lambda_t=0.141$

With the decreasing gap ratio, the flow structure is qualitatively similar when  $G > 0.06$ . When the gap ratio is further reduced to 0.02, a Stewartson flow structure appears in mid and high radius area. It is obviously reflected in the difference showed in Fig. 9 where  $r/b > 0.8$ .

With a summarization of data, the sphere of application of the temperature distribution calculated by flow structure is showed in Table 4. If the adiabatic wall temperature distribution of the

rotor in real turbine machines which can be the temperature boundary conditions to analyze convection heat transfer can't be obtained.

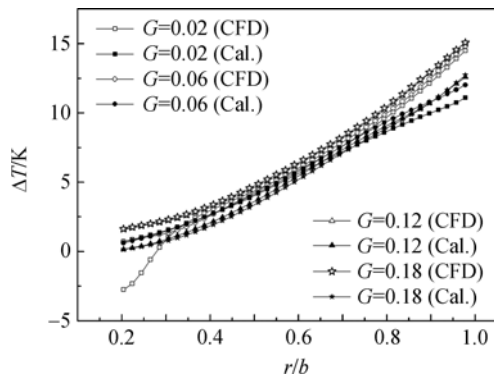


Fig. 9 Comparison results of temperature distribution by CFD method in case of  $\lambda_t = 0.141$

**Table 4 Applicable condition of method to calculate the temperature distribution**

G	0.06	0.12	0.18
$\lambda_t$	0.170~0.24	0.141~0.236	0.141~0.236

As the temperature rise distributions which meet the applicable condition is not sensitive with the influence of different gap ratios, the distribution calculated by tangential velocity distribution is also can be derived approximately with the swirl ratio  $\beta$  of the flow core.

The swirl ratio  $\beta$  distribution along the radius is showed in Fig. 10 with a suitable condition of  $\lambda_t \geq 0.14$  and  $G \geq 0.06$ . If the data at low radial ( $r/b < 0.4$ ) position can be ignored because of a weak windage heating effect, an appropriate constant value could substitute for the distribution curves of  $\beta$  to calculate the recovery temperature approximately in different situations. The approximate constant swirl ratio is listed in Table 5.

**Table 5 Approximate constant swirl ratio**

G	0.06	0.12	0.18
$\beta$	0.0790	0.0793	0.0824

With an approximate constant swirl ratio, the temperature rise can be calculated with the equation derived from Eq. (2)

$$\Delta T = r_{rev} \frac{\omega^2 (1 - \beta)^2}{2 c_p} r \quad (5)$$

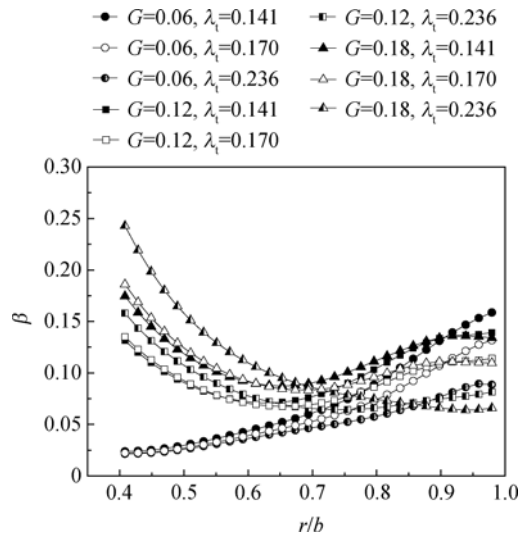


Fig. 10 Comparison results of  $\beta$  radial distribution by CFD method in case of  $G \geq 0.06$  and  $\lambda_t \geq 0.14$

Fig. 11 shows the temperature distribution calculated by Eq. (5), and compares it with the CFD results and theoretical calculated results from Eq. (2) in case of the gap ratio  $G = 0.12$ .

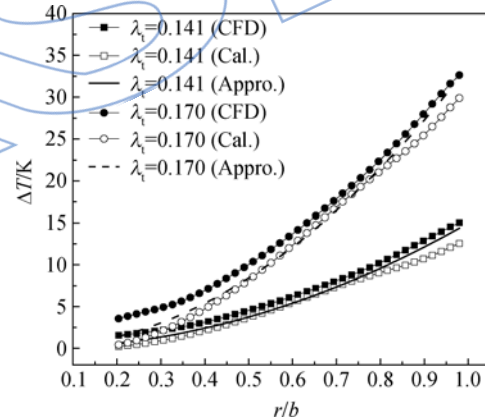


Fig. 11 Comparison results of temperature rise distribution calculated by approximate constant swirl ratios, CFD and theoretical calculation in case of  $G = 0.12$

Comparing the temperature rise distribution obtained by numerical method and the one calculated approximately with a constant swirl ratio shown in Fig. 11, error margin is within the scope of acceptable, especially in high radial position. This approximate method may be more widely used in a practical application because the swirl ratio would be more easily to get than tangential velocity distribution within an unfamiliar shrouded rotor-stator cavity system.

### 3 Conclusion

The rotating disk surface temperature rise owing to viscous friction effect has been obtained by CFD. In order to testify the accuracy of the CFD results, PIV experiments have been conducted to compare the velocity distributions. Besides, the high speed airflow recovery temperature calculation method has been tested to estimate the rotor surface temperature rise using the velocity differences between the rotor surfaces and rotating fluid core within a rotor-stator cavity system. Results from two methods have been compared under several conditions.

When  $G > 0.06$ ,  $0.141 < \lambda_t < 0.236$ , the high speed airflow recovery temperature equation predicts the temperature rise pretty well. It is safe to estimate the windage temperature rise via the recovery temperature equation using the velocity differences between the rotor surface and the rotating flow core. The analysis of flow structure using streamline chart indicates the agreement of two methods in solving temperature distribution. If there is a lack of inflow rate, the flow structure in the cavity is heavily influenced by the shroud, which would lead to a overheating of the rotating disk and low velocity of flow core in high radial position.

For practical application, the distribution of temperature would be estimated with an approximate constant swirl ratio within the margin of error. It simplifies the process because the flow velocity distribution may be not easily obtained.

### References:

- [1] Daily J W, Nece R E. Chamber dimension effects on induced flow and frictional resistance of enclosed rotating disks[J]. Journal of Basic Engineering, 1960, 82(1): 217-230.
- [2] Bayley F J, Owen J M. The fluid dynamics of a shrouded disk system with a radial outflow of coolant[J]. Journal of Engineering for Power, 1970, 92(3): 335-341.
- [3] Owen J M. The effect of forced flow on heat transfer from a disc rotating near a stator[J]. International Journal of Heat and Mass Transfer, 1971, 14(8): 1135-1147.
- [4] Bayley F J, Owen J M. Flow between a rotating and a stationary disc[J]. Aeronautical Quarterly, 1969, 20: 333-354.
- [5] Owen J M, Haynes C M, Bayley F J. Heat transfer from an air-cooled rotating disk[J]. Journal of Mathematical and Physical Science, 1974, 336(1607): 453-473.
- [6] Bayley F J, Long C A, Turner A B. Discs and drums: the thermo-fluid dynamics of rotating surfaces[J]. Journal of Mechanical and Engineering Science, 1993, 207(2): 73-81.
- [7] Coren D, Childs P R N, Long C A. Windage sources in smooth-walled rotating disc systems[J]. Journal of Mechanical Engineering Science, 2009, 223(4): 873-888.
- [8] Childs P R N, Noronha M B. The impact of machining techniques on centrifugal compressor impeller performance [J]. Journal of Turbomachinery, 1999, 121(4): 637-643.
- [9] Liu H P, Werst M, Hahne J J, et al. Prediction of windage losses of an enclosed high speed composite rotor in low air pressure environments[R]. ASME Paper HT2003-47118, 2003.
- [10] Da Soghe R, Facchini B, Innocenti L, et al. Analysis of gas turbine rotating cavities by an one-dimensional model[R]. ASME Paper GT2009-59185, 2009.
- [11] Childs P. Flow in rotating components-discs, cylinders and cavities[R]. Denver: IHS Global, 2007.
- [12] Poncet S, Chauve M P, Schiestel R. Batchelor versus Stewartson flow structures in a rotor-stator cavity with throughflow [J]. Physics of Fluids, 2005, 17(7): 075110. 1-075110. 15.
- [13] Batchelor G K. Note on the class of solutions of the Navier-Stokes equations representing steady rotationally symmetric flow[J]. Quarterly Journal of Mechanics and Applied Mathematics, 1951, 4(1): 29-41.
- [14] Lewis L V. In-engine measurements of temperature rises in axial compressor shrouded stator cavities[R]. ASME Paper GT2002-30245, 2002.
- [15] Lewis L V, Provins J I. A non-coupled CFD-FE procedure to evaluate windage and heat transfer in rotor-stator cavities[R]. ASME Paper GT2004-53246, 2004.